Space Object Tracking from the Robotic Optical Observatory at RMIT University

Steve Gehly
RMIT University, now at UNSW Canberra, Australia
Brett Carter, Yang Yang, Han Cai, Samantha Le May, Robert Norman
RMIT University and SERC Limited, Melbourne, Australia
Julie Currie, Bill Adamos
RMIT University, Melbourne, Australia
Jérôme Daquin
RMIT University, now at University of Padova, Italy
Richard Linares
Massachusetts Institute of Technology, Cambridge, MA, USA
Vishnu Reddy
Lunar and Planetary Lab, University of Arizona, Tucson, AZ, USA

ABSTRACT

The proliferation of space debris in recent decades has driven the aerospace research community to develop novel methods of data collection, fusion, and statistical inference in order to catalog and characterize the growing population of objects. This research is often facilitated by affordable, small-aperture telescopes that allow universities and other institutions to develop and test new algorithms to achieve space situational awareness objectives. This paper describes the installation of a new 0.4m telescope at RMIT University near Melbourne, Australia, as part of a joint project with researchers at the Massachusetts Institute of Technology and University of Arizona. An overview of the system hardware and software is provided, as well as the results of photometric data analysis from the first operational campaign conducted earlier this year. The paper further outlines opportunities for STEM outreach with local schools and concludes with a discussion of next steps and future research applications to be undertaken with the telescope.

1. INTRODUCTION

One of the key challenges facing researchers in space situational awareness (SSA) is the lack of available data to develop and test solutions for various SSA objectives, including orbit determination, track correlation, object characterization, and sensor management. Institutions with access to telescope and radar data have a distinct advantage in pursuing these topics, enabling them to produce meaningful research while also facilitating student development and community outreach. A number of universities and research institutions have deployed telescopes in recent years for the express purpose of conducting SSA research [1–3]. Networks such as the International Scientific Optical Network (ISON) [4], Falcon Telescope Network [5, 6], and SMARTnet [7, 8] enable further capabilities in cataloging and characterizing the growing population of objects in Earth orbit.

Recent work has demonstrated the ability of low-cost, small aperture telescopes to perform useful research in space situational awareness. The Optical tracking and Spectral characteriztation of Cubesats for Operational Missions (OSCOM) system developed at Embry-Riddle University cost only $10K and is capable of producing high rate photometric measurements of cubesats in Low Earth Orbit in order to estimate spin rates [2]. Similar experiments have been conducted with the Swisscube and Buccaneer cubesats, in which observations were compared against telemetry downlinked from the spacecraft [9, 10]. Another low-cost optical system, Tracker Of Things In Space (TOTIS), was developed by the Defence Science and Technology Group (DSTG) in Australia to solve the joint search and track sensor management problem, allowing for the automated build-up and maintenance of a space object catalog [3]. Across numerous other institutions and applications, similar projects have facilitated the development of innovative solutions to challenging problems in SSA.

This paper provides an overview of the recently constructed Robotic Optical Observatory (ROO) hosted at RMIT University in Melbourne, Australia. In partnership with the Massachusetts Institute of Technology and University of Arizona, the 0.4m telescope is primarily intended for SSA research, in particular to gather astrometric and photometric data for objects in geosynchronous Earth orbit (GEO). By providing complementary data to sensors in North America, the ROO telescope enables collaborative research on space objects across the GEO belt. The paper is organized as follows. Section 2 provides a detailed description of the observatory hardware, software, location, and operations. Section 3 describes the results of the first observations collected with the telescope. Section 4 highlights additional applications including community outreach and Science, Technology, Engineering, and Mathematics (STEM) engagement with primary and secondary schools. Finally, conclusions and proposals for future research are included in Section 5.

2. SYSTEM OVERVIEW

2.1. HARDWARE DESCRIPTION

The main instrument is a 16-inch Starizona Hyperion Astrograph mounted on a Sotware Bisque Paramount ME II (Fig. 1). The telescope is a Cassegrain reflector based on the Harmer-Wynne optical design, which uses a parabolic primary mirror, spherical secondary mirror, and a doublet lens to correct the comatic aberration and astigmatism introduced by the mirror pair [11]. The telescope is equipped with a focal reducer that converts the focal ratio from f/7.3 to f/5.2. The main camera is a monochrome Atik 16200 charge-coupled device (CCD), with 6-μm square pixels in a 4499x3599 array, which results in a field of view (FOV) of 0.73x0.59 degrees with the reduced focal ratio. A color version of the same camera has recently been purchased for astrophotography and STEM outreach applications, as discussed in Section 4. A secondary guider telescope and camera are mounted on top of the main telescope to assist with target acquisition and additional data collection. The entire assembly is housed in a fully automated 3m dome with a retractable shutter and rotating base. A full summary of system specifications is provided in Table 1.

(a) 16-inch Hyperion Astrograph on Paramount ME II (b) Full Hardware Setup

Fig. 1. Robotic Optical Observatory Hardware

Table 1. System Specifications

Main Telescope	Starizona Hyperion	Main Camera	Atik 16200 CCD
Aperture	16-inch (406 mm)	Pixel Size	6 μm x 6 μm
Focal Length	2960 mm	Array Size	4499 x 3599 pixels
Focal Ratio	f/7.3 (f/5.2 with focal reducer)	FOV Size	0.52° x 0.42° (0.73° x 0.59° with focal reducer)
Guider Telescope	Orion ShortTube 80 OTA	Guider Camera	Starlight Xpress Lodestar X2
Aperture	80 mm	Pixel Size	8.2 μm x 8.4 μm
Focal Length	400 mm	Array Size	752 x 580 pixels
Focal Ratio	f/5	FOV Size	0.92° x 0.68°

2.2. LOCATION AND INSTALLATION

The observatory is located at RMIT University's Bundoora Campus, on the roof of Building 201 as shown in Figure 2 and with coordinates provided in Table 2. The location is approximately 20km northeast of Melbourne city center, providing some reduction in the background light pollution. The view is partially obstructed by a brick wall to the west, as seen in the inset of Fig. 2 and Fig. 3; however, the telescope has an otherwise unobstructed view to the north, in particular, to the GEO belt.

Table 2. Location Parameters

Latitude	Longitude	Height
37.68° S	145.06° E	172.4 m

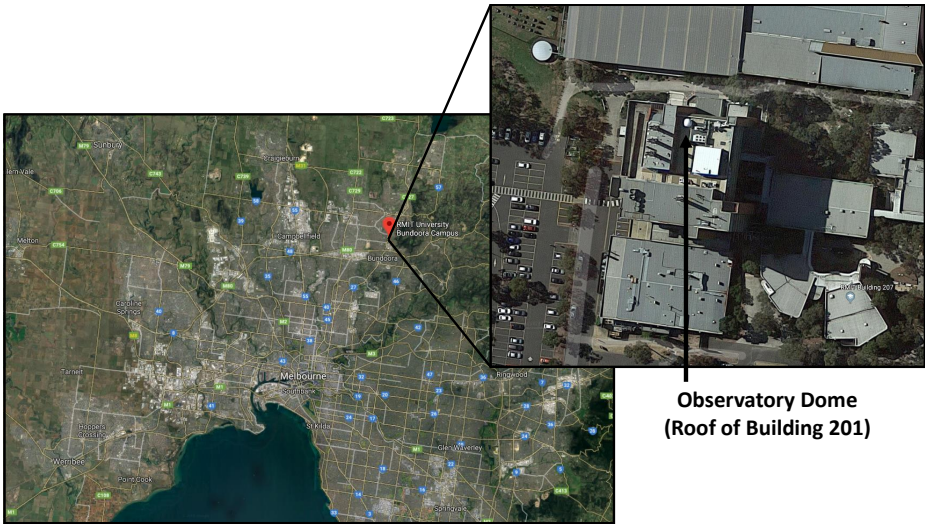

Fig. 2. Observatory location in Bundoora, VIC, approximately 20km northeast of Melbourne.

Fig. 3. ROO Crew, from left: J. Daquin, J. Currie, Y. Yang, S. Gehly, R. Norman, S. Le May, H. Cai

Installation of the observatory was completed in October 2017, with the assistance of multiple staff and graduate students (Fig. 3). The ScopeDome 3m dome required two days to assemble and is fixed to the concrete slab with a series of bolts. The telescope mount is attached to a 24-inch pier fixed to the slab with four bolts. Power and data connections are run through conduits in the slab to the equipment inside. The observatory is equipped with a weather station and uninterruptible power supply to support remote and automated operations. In the event of bad weather or a loss of power, the system will execute a shutdown procedure and close the dome.

2.3. OPERATIONS

At this stage in the project, observations are collected manually onsite or through remote login to the observatory computer. TheSkyX software package produced by Software Bisque is used to connect to and operate all equipment, including the dome, mount, and cameras. At the beginning of an observation session, a set of Two Line Element (TLE) data is downloaded for all objects to observe that night. After loading the data into TheSkyX, objects can be observed in satellite tracking mode, in which the telescope follows along the satellite orbit and stars appear as streaks in the background of camera images, or they can be observed in sidereal tracking mode, in which stars show up as points and objects streak across the image. The former case is more useful for photometric data analysis, while the latter is more suited to astrometric measurements to be used in orbit determination.

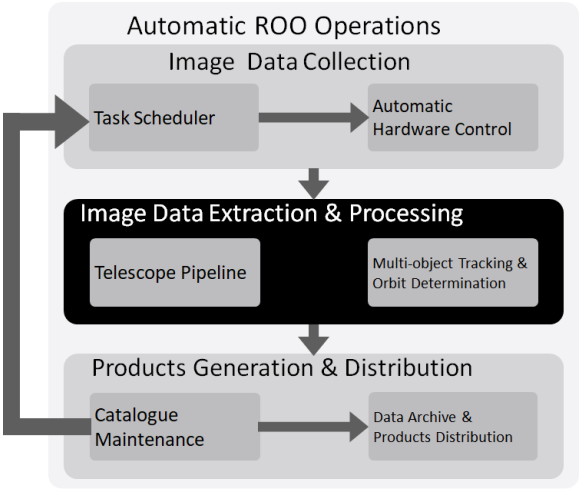

Fig. 4. Automation Architecture

Work is currently underway to automate operation of the observatory, first to allow users to schedule lists of objects to observe in advance of sessions, and ultimately to allow automated scheduling by the observatory software to produce data needed to achieve research objectives in orbit determination and object characterization, similar to the TOTIS system [3]. The overall software architecture of the system is presented in Fig. 4. When and where possible, the observatory will be tasked to collect data complementary to partner organization research objectives, such as performing simultaneous observation of UNSW Canberra cubesats with Falcon network telescopes.

3. FIRST OBSERVATION CAMPAIGN RESULTS

3.1. FIRST LIGHT

The first satellite image collected from the telescope was of the National Broadband Network (NBN) Skymuster 1, as seen in Fig. 5, on 2018-01-16. The telescope was operated in sidereal tracking mode, such that stars show up as points and satellites streak across the image. In the figure, the streak closest to the right is the Skymuster satellite, with two additional satellites also captured in the field of view. The Flexible Image Transport System (FITS) file was processed in AstroImageJ [12] and plate solved using astrometry.net to produce accurate astrometric locations for all objects in the image; stars used for this solution are indicated in Fig. 5(a). Fig. 5(b) plots the location of the NBN Skymuster satellite (NORAD 40940) in topocentric spherical coordinates along with several nearby objects. Additionally, the field of view is indicated by a dashed line allowing for visual identification of the objects captured in the image.

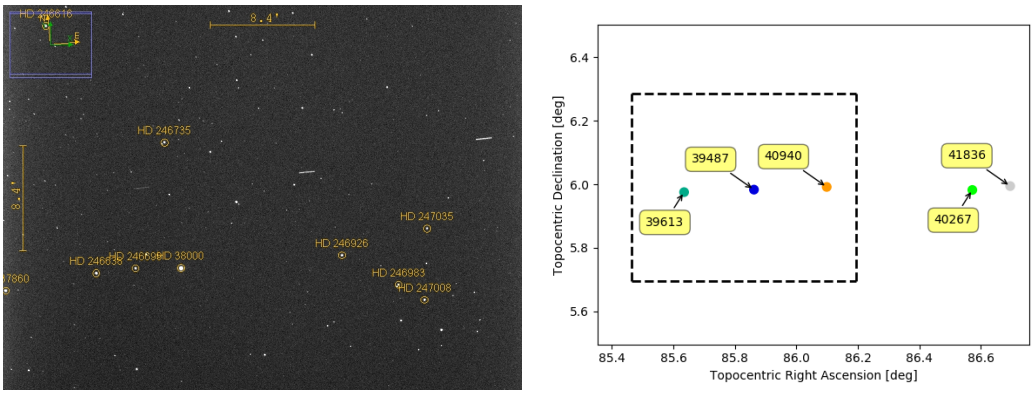

(a) First Image

(b) TLE Data in Measurement Space

Fig. 5. a.) First satellite image collected 2018-01-16 12:43:20 UTC. NBN 1A Skymuster (NORAD 40940) appears as streak to far right of image. Additional streaks correspond to EXPRESS AT-2 (NORAD 39613) and EXPRESS AM-5 (NORAD 39487). Stars used for astrometric solution indicated in yellow. b.) TLE data mapped to topocentric measurement space at this time depicting Skymuster and nearby objects. FOV is indicated by dashed line allowing for identificaiton of objects in image.

3.2. GEO PHOTOMETRY CAMPAIGN

As a first application for the observatory, a set of six objects in GEO and geostationary transfer orbit (GTO) were observed on the nights of April 19-21, 2018. The objects included active and inactive satellites and a rocket body, and the telescope was commanded to track each object along its orbit for a period of ten minutes, using the TLE as the initial state estimate. After cycling through all objects, the schedule was repeated to collect a total of three passes for each object. On the night of April 20, 2018, the Falcon telescope at UNSW Canberra was commanded to observe the same objects simultaneously, allowing for comparison of the lightcurves generated at each location. This section presents a subset of the lightcurves generated from the dual collection, for the objects listed in Table 3.

Table 3. Osculating Orbital Elements at Epoch

Object	NORAD ID	Orbit	Classification	a [km]	e	i	Ω	ω	M
Eutelsat 2-F1	20777	GEO	Inactive Satellite	42425.8	3.63e-4	14.3°	22.4°	−98.6°	202.6°
Optus D1	29495	GEO	Active Satellite	42166.4	3.34e-4	0.071°	103.5°	−72.1°	96.8°
Optus 10	40146	GEO	Active Satellite	42166.3	1.23e-4	0.052°	83.6°	−43.9°	88.9°
Ariane5 R/B	42816	GTO	Rocket Body	24338.4	0.728	2.77°	−44.7°	45.4°	41.3°

To collect images for photometric analysis, the telescopes were operated in satellite tracking mode, using the TLEs to follow each object along its orbit. Fig. 6 provides a sample image for each telescope tracking Eutelsat 2-F1 at approximately the same time. In both images, the object appears as a point with background stars captured as streaks. The Falcon telescope has a significantly smaller field of view, approximately 0.18 degrees on each side, which accounts for the difference in scale between the images and the number of stars present.

Fig. 7 presents the first set of dual-collect lightcurves from the ROO and Falcon telescopes. In all cases, the images were processed using AstroImageJ to compute the signal to noise ratio (SNR) at each time. Higher values of SNR indicate points of increased brightness relative to the background noise; sharp peaks indicate specular glints from various surfaces of the spacecraft. The FITS file headers contain timestamps in UTC for each image. The timestamps have been used to generate a common time axis for the data from each telescope, measured in seconds from the start of the pass, which allows for direct comparison of the SNR values.

Fig. 7(a) provides the lightcurves for Eutelsat 2-F1, in which several features are apparent. The overall trend in both the ROO and Falcon data is decreasing with periodic peaks corresponding to specular glints. There is good temporal agreement between the datasets, though there are some differences in the relative intensity of glints, possibly

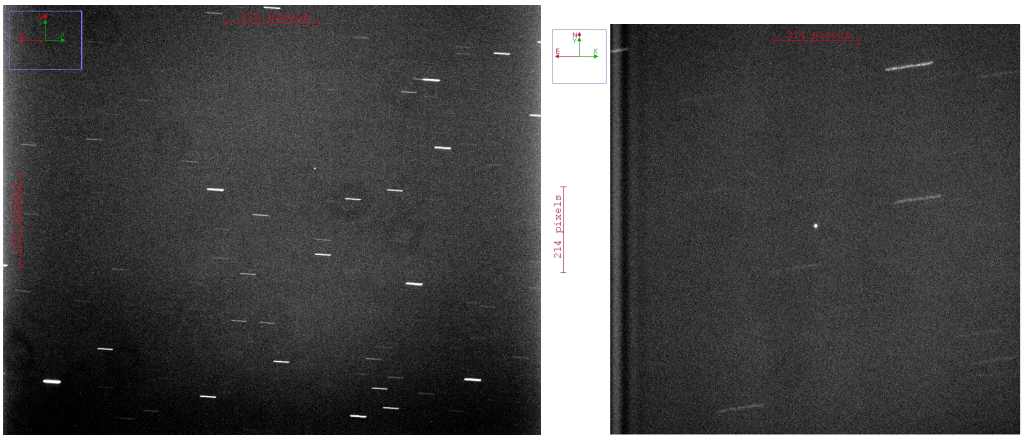

(a) ROO Image (b) Falcon Image

Fig. 6. Dual-Collect Images of Eutelsat 2-F1

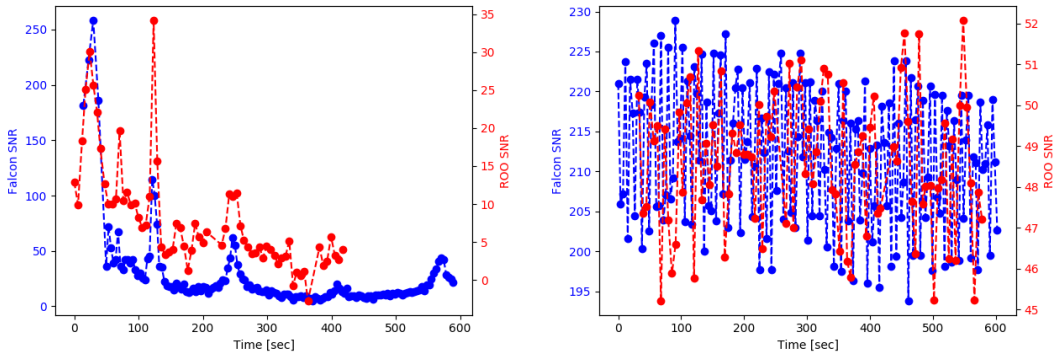

(a) Eutelsat 2-F1 (b) Ariane 5 Rocket Body

Fig. 7. Dual-Collect Lightcurves of Eutelsat 2-F1 and Ariane 5 Rocket Body

due to the differences in observation geometry between the two sites. The highest peaks occur around 30 and 120 seconds, though regular peaks continue for the remainder of the pass. There is also a smaller peak at approximately 70 seconds, most clearly visible in the ROO data. The large peaks likely correspond to reflections from the solar panels while smaller peaks are produced by glints from the spacecraft body. The overall profile suggests a slow rotation, the time between later glints is approximately 160 seconds. If these represent body panels 90 degrees apart, the apparent rotation rate wihtout correcting for orbital motion is a little over 0.5 degrees per second.

One clear difference between the datasets is the amplitude of the SNR for each telescope. For most of the pass, the Falcon data SNR is approximately 4-5 times higher than the ROO data SNR. This could be due to several factors, including the location of the sensors, the physical dimensions of the telescopes, and the use of filters. The USNW Falcon is located in an empty field away from urban areas and light pollution, and is at nearly 500m higher altitude, reducing the effects of atmospheric attenuation. Additionally, the Falcon telescope aperture is 10cm larger, allowing it to collect more light, and the images were taken using an exoplanet filter while ROO images were collected with no filter. As seen in subsequent figures, the difference in SNR is consistent across multiple objects throughout the observation session.

In contrast to the Eutelsat data, the Ariane 5 rocket body lightcurves show a great deal of variation from one image to the next, but without any large, clearly defined peaks. The average SNR values are significantly higher than for Eutelsat, indicating the rocket body is much brighter. While the variations could correspond to specular glints and rotation as before, the peaks are only 10-15 seconds apart. The rocket body is shaped like a cylinder, with a small cone

on one end. The observed frequency of glints produces an apparent rotation of 6-9 degrees per second if the object is spinning end over end. If it is instead rotating about its centerline, the lightcurve could result from a much slower rotation with regular glints caused by features on the surface. Dimensions obtained from ESA's DISCOS database [13] confirm that the cylinder is oblate, so this would correspond to a stable rotation and is therefore considered the most probable explanation.

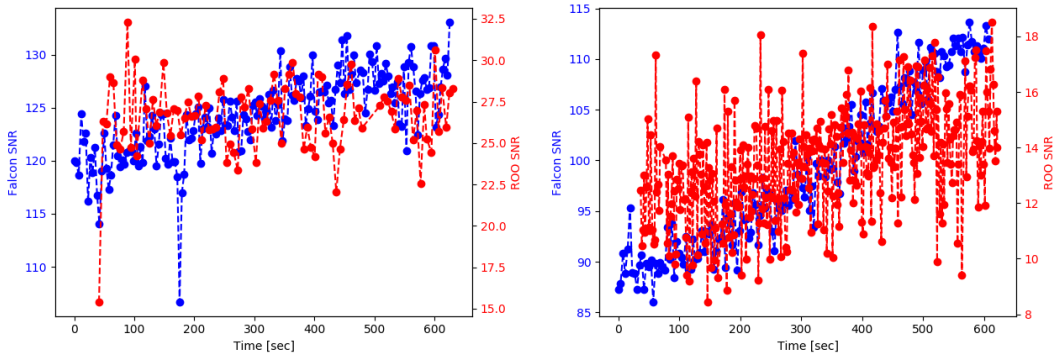

(a) Optus 10 (b) Optus D1

Fig. 8. Dual-Collect Lightcurves of Optus 10 and Optus D1 Satellites

Fig. 8 provides lightcurves for two active GEO communications satellites, Optus 10 and D1. Comparing the two subfigures, the SNR for Optus 10 is higher, which is reasonable because it is a larger spacecraft as confirmed by dimensions in DISCOS. In the Optus 10 lightcures (Fig. 8(a)), the most distinctive feature is a sharp drop in SNR occurring about 120 seconds apart in the ROO and Falcon data. The cause of this feature is unclear and could simply be a data outlier, but it may also be a result of self-shadowing with some portion of the spacecraft body or a deployable structure momentarily blocking sunlight from reaching other reflective surfaces. The difference in time could result from the different observing geometry at the two sites. The SNR for both telescopes exhibits a slight upward trend over the course of the pass, though the effect is more pronounced in the Falcon data. In the Optus D1 lightcurves (Fig. 8(b)), the upward trend is significantly larger in the SNR of the Falcon data as compared to ROO. Because they are actively controlled geostationary spacecraft, both satellites maintain a fixed location and orientation relative to the ground. As such, slow trends in the lightcurves are most likely due to changing solar phase angle as the Earth rotates and the spacecraft proceeds in its orbit.

To illustrate this effect, the analytical equations for the flux, F_{diff}, and apparent magnitude, m_{app}, of a diffuse sphere as a function of phase angle are included [14]:

$$F_{\text{diff}}(a_0, r_{\text{sat}}, \phi) = \frac{2}{3} a_0 \frac{r_{\text{sat}}^2}{\pi R^2} [\sin\phi + (\pi - \phi)\cos\phi] \tag{1}$$

$$m_{\text{app}} = -26.74 - 2.5 \log_{10}(F_{\text{diff}}) \tag{2}$$

where a_0 is the albedo, r_{sat} is the radius of the satellite, R is the range from satellite to ground station, and ϕ is the solar phase angle between the sun-satellite-observer.

Fig. 9 shows the variation in magnitude and flux as a function of phase angle for a 1 meter radius sphere with $a_0 = 0.2$ at GEO. While this is not an accurate description of the expected flux or magnitude of the Optus satellites, it does illustrate the effect of solar phase angle on brightness. Namely, as the solar phase angle approaches zero, the flux increases and the magnitude decreases, corresponding to an increase in brightness. Therefore, the highest expected SNR values in the telescope data are expected to occur around local midnight, when the solar phase angle is smallest. Because the observations were taken prior to midnight, the solar phase angle is decreasing during the pass, leading to an expected increase in brightness as a result. This simplified analysis agrees with the presentation of data from real GEO spacecraft in [14].

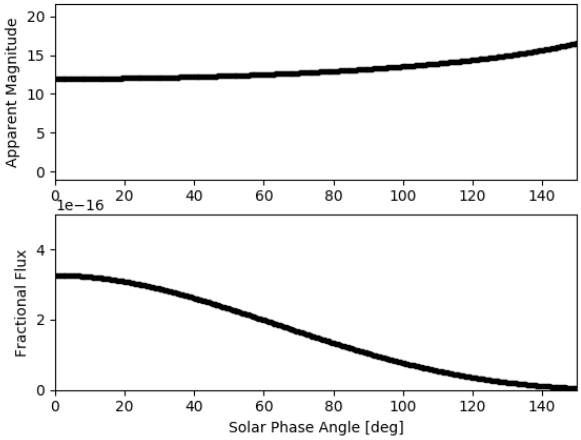

Fig. 9. Magnitude and Flux for Diffuse Sphere at GEO

4. ASTROPHOTOGRAPHY AND STEM OUTREACH

In addition to SSA applications, the observatory provides an ideal opportunity to do community outreach in science and engineering, and in particular, to promote STEM education in local primary and secondary schools. An important goal of the project is to develop and implement a process by which teachers and students can propose objects to observe, modeled after the Falcon Telescope Network's First Light project. ROO operators can work with students to refine requests and ensure they are feasible and sufficient to achieve the desired outcomes. In addition, the group can host viewing parties open to the community and other departments at RMIT to encourage collaboration and interest in astronomy and science more broadly. In support of these activities, the observatory can be used to collect images of astonomical objects of interest, including planets, galaxies, and nebulas, as depicted in Fig. 10.

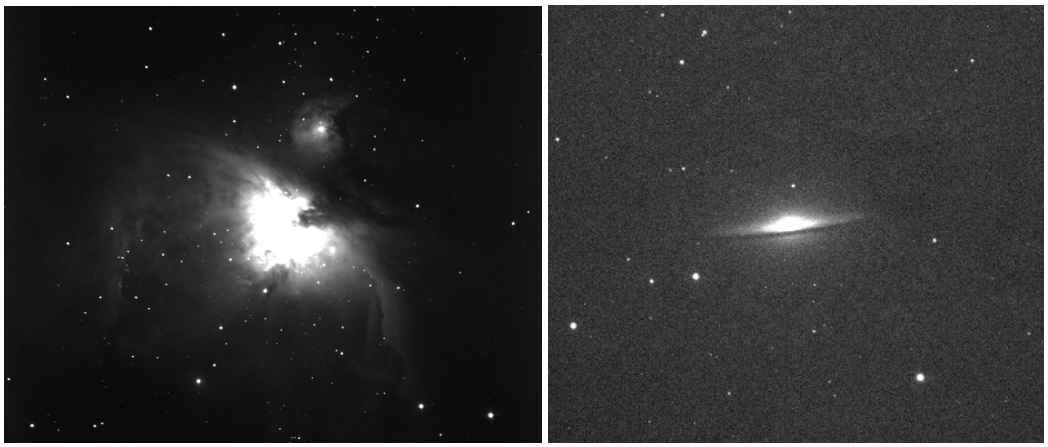

(a) Orion Nebula (b) Sombrero Galaxy

Fig. 10. Astrophotography Images

5. CONCLUSIONS AND FUTURE WORK

This paper provided a detailed description and initial results from the newly installed Robotic Optical Observatory in Melbourne, Australia. Comparisons of photometric data between ROO and the UNSW Canberra Falcon telescope

showed good agreement, and allowed for the inference of spin rates associated with inactive space objects. Observations of active spacecraft were further shown to follow expected trends in changing brightness as a function of solar phase angle. Use of the telescope is not limited to tracking objects in Earth orbit, and plans are currently being developed to work with local schools to promote STEM education.

A number of tasks remain to transition the observatory to fully automated operation. Software is being developed and tested to compute astrometric and photometric measurements from images in order to streamline data processing. Previous research by the authors has examined methods to correlate tracklets to perform data association and initial orbit determination, which would make ideal research applications for the telescope. In addition, when the system is fully automated and able to compute orbits from data, it will be possible to develop and test higher level algorithms to perform sensor management, object characterization, and event detection. Ultimately, the objective is for the observatory to facilitate the development and testing of novel algorithms to perform autonomous collection and exploitation of data for objects in the near Earth space environment.

6. ACKNOWLEDGMENTS

The authors wish to acknowledge UNSW Canberra and the US Air Force Academy Falcon Telescope Network for providing resources and data to perform photometry comparisons. Funding for this project was provided through the RMIT Capital Expenditure (CAPEX) program in addition to contributions by the Massachusetts Institute of Technology.

7. REFERENCES

1. Ryan D. Coder and Marcus J. Holzinger. Multi-objective design of optical systems for space situational awareness. *Acta Astronautica*, 128:669–684, 2016.

2. Forrest Gasdia, Aroh Barjatya, and Sergei Bilardi. Time-resolved cubesat photometry with a low cost electro-optics system. In *Advanced Maui Optical and Space Surveillance Technologies Conference*, Maui, HI, September 2016.

3. Nicholas Moretti, Mark Rutten, Travis Bessell, and Brittany Morreale. Autonomous space object catalog construction and upkeep using sensor control theory. In *Advanced Maui Optical and Space Surveillance Technologies Conference*, Maui, HI, September 2017.

4. I. Molotov, V. Agapov, V. Kouprianov, V. Titenko, V. Rumyantsev, V. Biryukov, G. Borisov, Yu. Burtsev, Z. Khutorovsky, G. Kornienko, A. Erofeeva, E. Litvinenko, A. Aliev, R. Zalles, O. Grebetskaya, Yu. Likh, O. Rusakov, N. Minikulov, M. Guliamov, B. Abdulloev, N. Borisova, T. Irsmambetova, A. Vikhristenko, R. Inasaridze, E. Gubin, A. Erofeev, Yu. Ivaschenko, V. Yurkov, A. Matkin, A. Rybak, D. Karaush, A. Letsu, O. Tsibizov, B. Ermakov, and E. Siniakov. ISON worldwide scientific optical network. In *Proceedings of the Fifth European Conference on Space Debris*, Darmstadt, Germany, March-April 2009.

5. Francis K. Chun, Roger D. Tippets, Michael E. Dearborn, Kimberlee C. Gresham, Ryan E. Freckleton, and Martin W. Douglas. The U.S. Air Force Academy Falcon Telescope Network. In *Advanced Maui Optical and Space Surveillance Technologies Conference*, Maui, HI, September 2014.

6. Francis K. Chun, Roger D. Tippets, David M. Strong, Devin J. Della-Rose, Daniel E. Polsgrove, Kimberlee C. Gresham, Joshua A. Reid, Casey P. Christy, Mark Korbitz, Joel Gray, Stanton Gartin, David Coles, Ryan K. Haaland, Russ Walker, Jared Workman, John Mansur, Victoria Mansur, Terry Hancock, Julia D. Erdley, Thomas S. Taylor, Richard A. Peters, Christopher X. Palma, William Mandeville, Steven Bygren, Christian Randall, Kevin Schafer, Tim McLaughlin, Jos Luis Nilo Castelln, Amelia Cristina Ramirez Rivera, Hector Andres Cuevas Larenas, Andrew Lambert, Manuel Cegarra Polo, David Blair, Mark Gargano, Jan Devlin, Richard Tonello, Carsten Wiedemann, Christopher Kebschull, and Enrico Stoll. A new global array of optical telescopes: The Falcon Telescope Network. *Publications of the Astronomical Society of the Pacific*, 130:095003:20pp, September 2018.

7. Hauke Fiedler, Martin Weigel, Johannes Herzog, Thomas Schildknecht, Marcel Prohaska, Martin Ploner, and Oliver Montenbruck. SMARTnet: First experience of setting up a telescope system to survey the geostationary ring. In *25th International Symposium on Space Flight Dynamics*, Munich, Germany, October 2015.

8. Hauke Fiedler, Johannes Herzog, Martin Ploner, Marcel Prohaska, Thomas Schildknecht, Martin Weigel, and Martin Klabl. SMARTnet (TM) - first results of the telescope network. In *Proceedings of the 7th European Conference on Space Debris*, 2017.

9. Jean-Noel Pittet, Jiri Silha, Thomas Schildknecht, Muriel Richard, Dimitri Hollosi Antal, Christophe Paccolat, Volker Gass, and Jean-Philippe Thiran. Space debris attitude determination of faint leo objects using photometry: Swisscube cubesat study case. In *Proceedings of the Seventh European Conference on Space Debris*, Darmstadt, Germany, April 2017.

10. M. Cegarra Polo, R. Abay, S. Gehly, A. Lambert, P. Lorrain, S. Balage, M. Brown, and C. Bright. Attitude detection of the Buccaneer Risk Mitigation Mission cubesat through experimental and simulated light curves in combination with telemetry data. In *Advanced Maui Optical and Space Surveillance Technologies Conference*, Maui, HI, September 2018.

11. C. F. W. Harmer and C. G. Wynne. A simple wide-field Cassegrain telescope. *Monthly Notices of the Royal Astronomical Society*, 177:25P–30P, 1976.

12. Karen A. Collins, John F. Kielkopf, Keivan G. Stassun, and Frederic V. Hessman. ASTROIMAGEJ: Image processing and photometric extraction for ultra-precise astronomical light curves. *The Astronomical Journal*, 153:77:13pp, February 2017.

13. T. Flohrer, S. Lemmens, B. Bastida Virgili, H. Krag, H. Klinkrad, E. Parilla, N. Sanchez, J. Oliveira, and F. Pina. DISCOS - current status and future developments. In *Proceedings of the Sixth European Conference on Space Debris*, Darmstadt, Germany, April 2013.

14. Rita L. Cognion. Observations and modeling of geo satellites at large phase angles. In *Advanced Maui Optical and Space Surveillance Technologies Conference (AMOS)*, Maui, HI, September 2013.